

EQUIVALENT LUMPED-ELEMENT CIRCUIT OF APERTURE AND MUTUALLY COUPLED CYLINDRICAL DIELECTRIC RESONATOR ANTENNA ARRAY

**Affan A. Baba¹, Mohd. A. Zakariya^{1, *}, Zuhairi Baharudin¹,
Muhd Z. U. Rehman¹, Mohd F. Ain², and Zainal A. Ahmad³**

¹Electrical and Electronics Engineering Department, Universiti Teknologi PETRONAS, Malaysia

²School of Electrical and Electronic Engineering, Universiti Sains Malaysia, Nibong Tebal, Penang 14300, Malaysia

³School of Materials and Mineral Resources Engineering, Universiti Sains Malaysia, Nibong Tebal, Penang 14300, Malaysia

Abstract—This paper presents an electrical model of aperture and mutually coupled three-elements cylindrical dielectric resonator antenna (CDRA) array designed for 802.11a system applications. In electrical model, each antenna component is represented by its equivalent RLC circuit. The advanced design system (ADS) software is used to build the electrical model and predict the behavior of return loss, while the antenna structure is simulated using CST microwave studio before fabrication. The first and last radiating elements of the proposed array are excited through the aperture slots while the middle element is excited through the mutual coupling of its neighboring elements. The slot length and inter-slot distance effects on bandwidth are comprehensively analyzed and presented. The maximum gain of the proposed array for 5.0 GHz band is about 10.8 dBi, and the achieved simulated (CST, ADS) and measured impedance bandwidths are 1.076 GHz, 1.0 GHz, and 1.2 GHz respectively. The proposed CDRA array antenna exhibits an enhancement of the gain (7.4%) and bandwidth (93.3%) as compared to a literature work with aperture slots. In this study, it is also observed that by using the mutual coupling instead of third slot to excite the middle CDRA, side lobe levels are also reduced significantly over the entire 5.0 GHz band.

Received 11 September 2013, Accepted 13 October 2013, Scheduled 18 October 2013

* Corresponding author: Mohd. Azman Zakariya (mazman.zakariya@petronas.com.my).

1. INTRODUCTION

Dielectric resonator antenna (DRA) technology has attracted many researchers. From literatures, the technology has been investigated since early 1980s after big contribution by Long et al. [1]. The DRA success is due to its several attractive features as compared to the conventional conductor antennas. The attractive characteristics of the DRA show that it can be a good radiating element. In addition, it can be implemented in various communication applications such as radars, satellite communication, wireless local area network (WLAN), and radio frequency identification (RFID).

Normally, single element DRA acts as a low gain antenna, but it has a broad radiation pattern. In some applications, high gain antennas are the major requirement for efficient long distance communication. Like conventional low gain antennas, DRA gain can also be enhanced by placing it in an array configuration. Several different shapes of DRAs have been proposed in the literatures i.e., cylindrical [2], rectangular [3] and triangular [4]. Among these shapes, cylindrical dielectric resonator antenna (CDRA) is widely used, due to its simple field structure as compared to rectangular DRA [5], and it is directional as compared to the rectangular and circular DRAs (i.e., rectangular and circular DRAs are bidirectional) [6]. The CDRA is characterized by its height h , radius a and permittivity ϵ_r as shown in Figure 1(a). Different types of feeding techniques have been proposed in the literatures to excite the DRAs arrays, such as probe feed, dielectric image guide, coplanar waveguide and microstrip transmission line. Among these different feeding techniques, the microstrip transmission line is more attractive due to low cost, small in size and ease of fabrication [7, 8]. In this proposed work, the microstrip transmission line feed is applied. It is characterized by its length L_s and width w_s as depicted in the Figure 1(b).

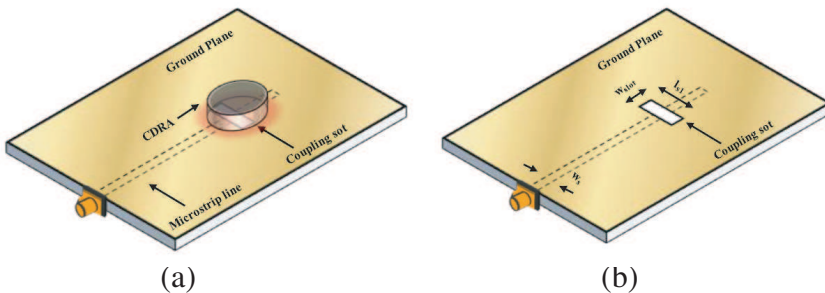


Figure 1. The geometry of the aperture coupled CDRA.

The main objective of this paper is to design a electrical model of high gain and wideband mutually coupled three-elements CDRA array for wireless LAN 802.11a applications. Subsequently, the proposed design is analyzed to obtain the antenna array performance through the development of the equivalent lumped-element circuit model. Then antenna array structure performance is analyzed using the CST microwave studio, advanced design system (ADS) and E8363C PNA vector network analyzer (VNA). The ADS lumped-element circuit is built to predict the behavior of return loss at required resonance frequency and verifies the antenna array feasibility.

2. CDRA ARRAY DESIGN METHODOLOGY

The geometry of single-element aperture coupled CDRA is depicted in Figure 1. It consists of CDRA with diameter $2a = 15$ mm, height $d = 3.0$ mm and permittivity $\epsilon_r = 55$. The coupling slot etched on the ground plane of FR4 substrate (1.565 mm thickness), with $\epsilon_s = 4.9$, is used to excite the CDRA through the $50\ \Omega$ microstrip transmission line. The aperture slot has a width w_{slot} and length l_{s1} of 4 mm and 14 mm, respectively. The single-element CDRA is used to design the aperture and mutually coupled CDRA array, excited by using a $50\ \Omega$ microstrip transmission line with a width of 2.6 mm, designed on the FR4 substrate with dielectric constant of 4.9 and a thickness of 1.565 mm as depicted in the Figure 2. The synthesis procedure is used to calculate the width of the transmission line. This proposed CDRA array consists of three elements of the same CCTO ($\text{CaCu}_3\text{Ti}_4\text{O}_{12}$) material used in the single element CDRA. The resonance frequency of CDRA for $TE_{011+\delta}$ is given as [9]:

$$f_0 = \frac{662.4 \times 10^6}{2\pi a \sqrt{\epsilon_{r+1}}} \left\{ 1 + 0.7013 \left(\frac{a}{d} \right) - 0.002713 \left(\frac{a}{d} \right)^2 \right\} \quad (1)$$

where: radius of CDRA, $a = 7.75$ mm. Height of CDRA, $d = 3$ mm. Dielectric constant, $\epsilon_r = 55$.

Two radiating elements of this proposed array (i.e., first and last CDRA) are excited through two aperture slots. These aperture slots of width $w_1 = w_2 = 4.0$ mm and length $L_1 = L_2 = 20$ mm are etched on the ground plane at a distance of $0.9\lambda_g$ and are excited through the microstrip transmission line. The third radiating element (i.e., the central CDRA) is excited through the mutual coupling of its neighboring elements. The distances between the consecutive elements are $0.264\lambda_{air}$ and $0.265\lambda_{air}$, respectively. From the literatures, it is clear that mutual coupling can be used to enhance the array performance [10]. In this proposed array, mutual coupling mechanism

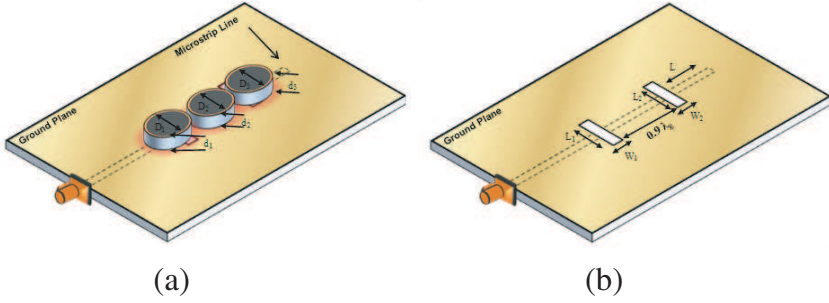


Figure 2. The geometry of the (a) CDRA array and (b) microstrip transmission line.

is used to enhance the bandwidth as well as gain. The effects of mutual coupling on the performance of proposed array are analyzed by designing the lumped-element circuit and are presented in the results section.

The open-ended stub matching mechanism is used for the impedance matching of loads and characteristic impedance of a microstrip transmission line. The purpose of impedance matching is to couple maximum amount of power to the antenna. Figure 2(b) shows that the length of the stub is L . The stub length L is selected such that it compensates the reactance impedance of the slot window. In [11], stub length initial value is given as:

$$L = \frac{\lambda_g}{4} \quad (2)$$

where λ_g denotes the guided wavelength. The value of λ_g is given as [11]:

$$\lambda_g = \frac{c}{f_0 \sqrt{\epsilon_s}} \quad (3)$$

where: c is the speed of light, f_0 the resonance frequency calculated from Equation (1), and ϵ_s the substrate permittivity.

The CST design showing the air gap between the CDRs and ground plane due to fabrication error (surface of the CDRs is not smooth) is depicted in Figure 3. The fabricated design of aperture and mutually coupled array antenna is depicted in Figure 4. This proposed array successfully achieves bandwidth from 4.8–6.0 GHz. The detailed dimensions of this CDRA array antenna are depicted in Table 1.

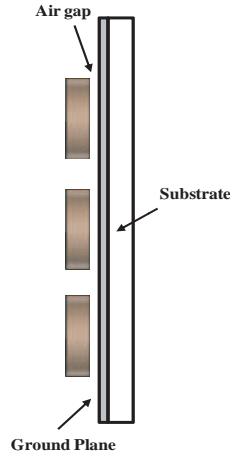


Figure 3. Prospective view of CDRA array to show the air gap between CDRs and ground plane.



Figure 4. The fabricated design of the aperture-coupled CDRA array. (a) Front view and (b) back view.

Table 1. Dimensions of aperture coupled CDRA array.

Parameters	Length (mm)
L_1, L_2	20.0
w_{slot}, w_1, w_2	4.0
D_1, D_2, D_3	15.5
d_1, d_2, d_3	3.0
w_s	2.6
L	$\lambda_g/4$
L_s	55

3. EQUIVALENT LUMPED-ELEMENT CIRCUIT

The aim of designing the lumped-element circuit is to analyze the aperture and mutually coupled antenna array performance at the desired frequency. Different steps have to be followed, and modeling the equivalent circuit is as follows.

3.1. Single Element Equivalent Circuit

To build the lumped-element circuit of the aperture coupled CDRA, the same technique is used as presented in [7]. An equivalent lumped-element circuit for single dielectric resonator is depicted in Figure 5. The resonant resistance, inductance and capacitance for the dielectric resonator are calculated using the expression found in [12].

$$R_r = \frac{2n^2 z_0 s_{11}}{1 - s_{11}} \quad (4a)$$

$$C_r = \frac{Q_0}{\omega_0 R_r} \quad (4b)$$

$$L_r = \frac{1}{C_r \omega_0^2} \quad (4c)$$

where s_{11} is the reflection coefficient, z_0 the characteristic impedance, Q_0 the quality factor, and n the coupling magnitude between excitation source and dielectric resonator. It is mentioned in [12] that the value of R_r is to be chosen properly because it makes an important contribution in determining the value of L_r and C_r .

The input impedance of the slot can be calculated using the

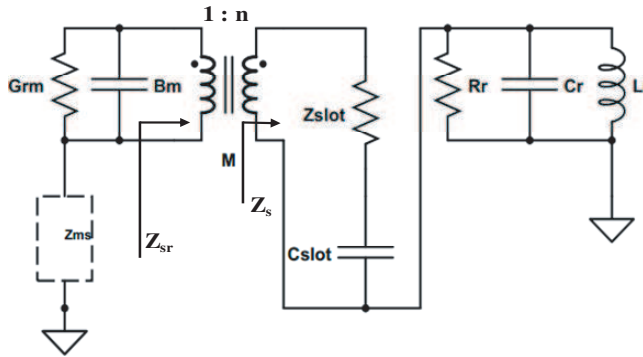


Figure 5. Equivalent circuit of aperture coupled DRA.

formulas found in [7] as:

$$Z_{slot} = Z_c \frac{2R}{1-R} + jZ_c \cot(\beta_f L_t) \quad (5)$$

where Z_c is the characteristic impedance of the transmission line, R the voltage reflection coefficient, β_f the propagation constant, and L_t the stub length. The input impedance of the transmission line can be calculated by using the expression presented in [13]:

$$G_{rm} = \frac{160\pi^2 h^2}{Z_{cm}^2 \lambda_0^2 \epsilon_{cm}} \quad (6a)$$

$$B_m = \omega C_l, \quad C_l = \frac{l_{eq} C \sqrt{\epsilon_{cm}}}{Z_{cm}} \quad (6b)$$

where h is the substrate height, Z_{cm} the characteristic impedance of the microstrip, E_{cm} the effective dielectric constant, l_{eq} the equivalent extra length of microstrip, and c the velocity of light. The input impedance, in series with the microstrip line is written as

$$Z_{sr} = n^2 Z_{slot} + \frac{n^2}{j\omega C_{slot}} + \frac{n^2 R_r}{1 + j\omega C_r R_r + \frac{R_r}{j\omega L_r}} \quad (7)$$

$$n^2 = \frac{Z_s}{Z_{sr}}$$

3.2. Mutually Coupled Array Antenna Equivalent Circuit

The novel four-elements aperture coupled array antenna has been introduced in [7] which does not include the coupling between the array elements because no wideband response was required. In our proposed work, the equivalent lumped-element circuit of aperture and mutually coupled array antenna in the improvisation of [7] is designed using ADS and depicted in Figure 6.

The mutually coupled array elements are connected by a coupling capacitor C_c due to the coupling between the dielectric resonators. As shown in the Figure 7, the total capacitance is the summation of gap capacitance in air (C_{air}), fringe capacitance C_{fringe} and overlapped capacitance $C_{overlapped}$. The expression used to determine the total capacitance is given as:

$$C_c = C_{air} + (2 * pi * r) * C_{fringe} + 2 * C_{overlapped} \quad (8)$$

C_{air} represents the coupling between the elements in air, C_{fringe} the capacitance from the edges of the CDR, and $C_{overlapped}$ is formed directly below the CDR, between CDR and ground plane.

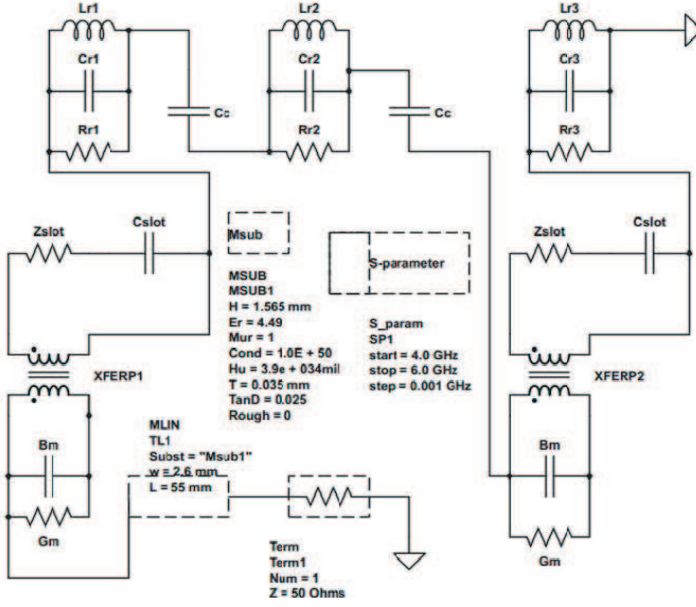


Figure 6. Equivalent lumped-element circuit of proposed array.

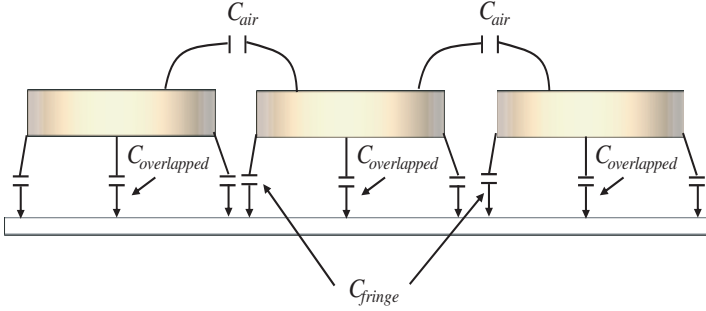


Figure 7. Coupling and fringe capacitance between the radiating elements.

3.2.1. Model for Air Gap Capacitance

The air gap capacitance between the array elements is calculated by using the equations as follows:

$$C_{air} = \begin{cases} \frac{\epsilon_0}{\pi} \ln \left\{ 2 \frac{1 + \sqrt{K'}}{1 - \sqrt{K'}} \right\}, & 0 \leq K^2 \leq 0.5 \\ \frac{\pi \epsilon_0}{\ln \left\{ 2 \frac{1 + \sqrt{K'}}{1 - \sqrt{K'}} \right\}}, & 0.5 \leq K^2 \leq 1 \end{cases} \quad (9)$$

where:

$$K' = \sqrt{1 - K^2} \quad (10)$$

In [14], using the rectangular shape design, the equation for constant 'K' is given as

$$K = \frac{S}{S + 2W} \quad (11)$$

In [15], width of the rectangular patch i.e., $w = 2r_0$ for the cylindrical type. Hence the design which applies cylindrical type, the equation for constant K is given as follows:

$$K = \frac{S}{S + 4r_0} \quad (12)$$

where S represents the distance between the elements, and r_0 is the radius of the cylindrical dielectric resonator.

3.2.2. Fringe Capacitance

The fringe capacitance between the dielectric resonators edges and ground plane is depicted in the Figure 7. The equation used to determine the fringe capacitance between the ground plane and CDR is given as

$$C_{fringe} = K_{av} * \epsilon_0 * \frac{(d + \alpha h) * 2 * r}{d} \quad (13)$$

where K_{av} is the average of dielectric relative permittivity between CDR layer and ground plane, α the factor to fix effective area $\{\alpha = (2r - d)/h\}$ for CDR, d the gap between dielectric resonator and ground plane (consider 0.2mm because the surface of the DR is not perfectly smooth), h the height, and r the radius of CDR.

3.2.3. Overlapped Capacitance

The overlapped capacitance between the overlapping area of CDR and ground plane is depicted in Figure 7. The equation used to determine the overlapped capacitance between the DRs and ground plane is given as

$$C_{overlapped} = K_{av} * \epsilon_0 * \left(\frac{A}{d}\right) \quad (14)$$

where K_{av} is average of dielectric relative permittivity, ϵ_0 the vacuum permittivity, A the overlap area, and d the distance between CDR and ground plane.

4. RESULTS AND DISCUSSION

The design specification of the single- and three-elements antenna array is built in CST. The complete geometries for the two antennas are depicted in Figure 1 and Figure 2. The steps in designing these antennas are carefully referred to the Equations (1) to (3). In addition, the equivalent lumped-element circuit is designed in the Advanced Design System (ADS) by applying Equations (4) to (14). Once these two stages are completed, the antennas are ready to be fabricated. The validity of the equivalent lumped circuit is judged by comparing the values of return losses obtained through the ADS against those obtained through the computer simulation technology (CST) and fabricated design measurements (using E8363C PNA vector network analyzer). The return loss (S_{11}) results obtained by the RLC model, CST design and voltage network analyzer (VNA) are in good agreement. The simulated (CST and ADS) and measured return losses of single-element CDRA are depicted in Figure 8. The simulated and measured bandwidths obtained through CST, ADS and fabricated designs are 0.2 GHz, 0.2 GHz, and 0.23 GHz, respectively. The equivalent circuit parameters for single element CDRA are depicted in Table 2.

Table 2. Parameters of equivalent lumped-element circuit.

Parameters	Values
R_r (Ω)	90.00
L_r (pH)	103.94
C_r (pF)	8.84
Z_{slot} (Ohms)	51.77
C_{slot} (pF)	0.54
B_m (TS)	6.15
G_{rm} (μ S)	31.54
Z_{ms} (Ω)	50.00

The return losses of the simulated and fabricated prototypes of the antenna array are depicted in Figure 9. The CST simulation gives the return loss of -51 dB at resonance frequency of 5.16 GHz with a bandwidth of 1.076 GHz. The ADS simulation gives the return loss of -51 dB at resonance frequency of 5.05 GHz with a bandwidth of 1.0 GHz, and the fabricated design with 1.2 GHz bandwidth and return

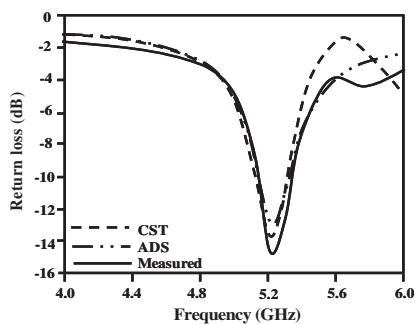


Figure 8. The comparison between the single element aperture coupled return loss results.

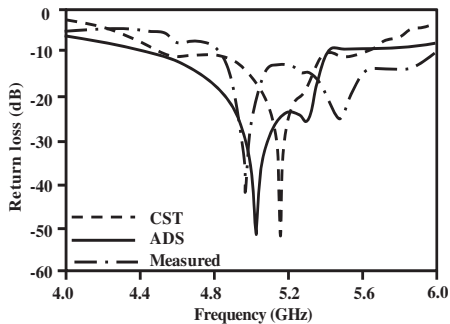


Figure 9. The comparison between the antenna array return loss.

loss of -42 dB give resonance at 5.0 GHz. The differences between the simulated and measured results are due to the fabrication losses (i.e., the surface of the CDRAs is not smooth and sticking of the elements on the exact position). The return losses results from the simulations and fabrication cover the required frequency band (5.15–5.825 GHz) for 802.11a application. The return loss results of the proposed array prove feasibility of the array antenna at the desired frequency.

A coupling slot length is varied to analyze its influence on the antenna bandwidth. As this antenna part is related to the feeding network, it has significant effects on antenna results. The initial slot lengths are chosen to be 2.0 mm and slot width chosen to be less than $\frac{\lambda_g}{4}$ to avoid the back radiation. The effects of the parametric study of slots length are depicted in Table 3, and it is clear that the best bandwidth is achieved at a slot length of 20.0 mm.

Table 3. Slot length analysis on antenna array bandwidth.

Slot length (mm)	Bandwidth (GHz)	Slot length (mm)	Bandwidth (GHz)
2.0	Null	14.0	0.636
4.0	0.0483	16.0	0.688
6.0	0.5130	18.0	0.742
8.0	0.4650	20.0	1.076
10.0	0.5180	22.0	0.594
12.0	0.5880	24.0	0.507

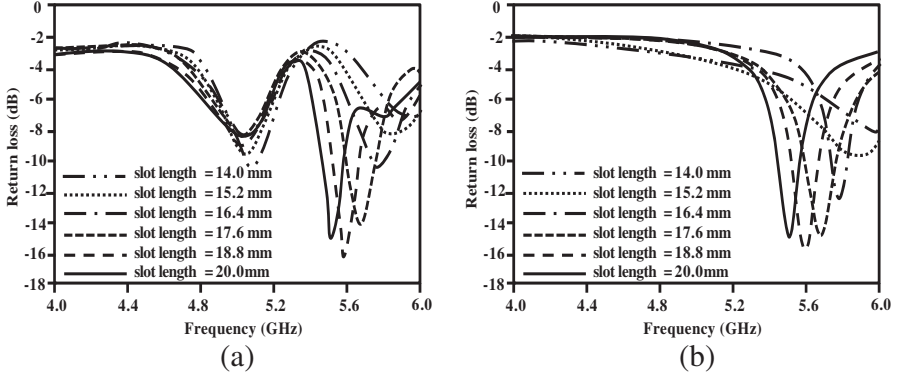


Figure 10. Slot length analysis on a first radiating element using (a) CST, (b) ADS.

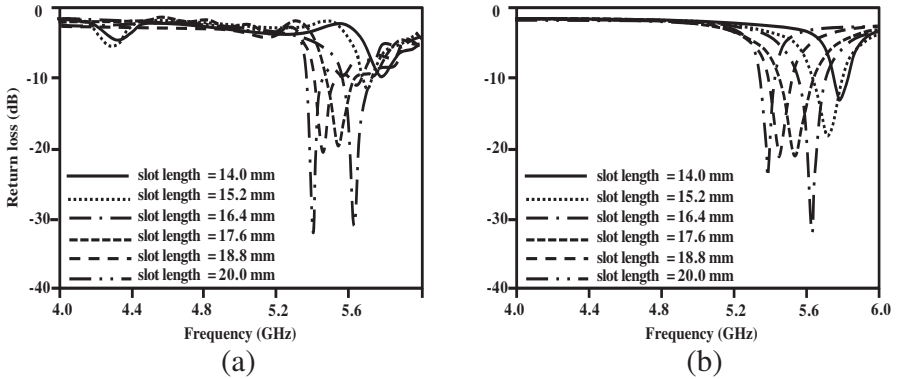


Figure 11. Slot length analysis on a last radiating element using (a) CST, (b) ADS.

The effects of changing the slot length on the return losses of the top radiating element, bottom radiating element and on complete array using CST and ADS software's are depicted in the Figure 10, Figure 11 and Figure 12, respectively. It is clearly shown that the CST and ADS show good and reasonable results which translate the functionality of the antenna design. The difference between the CST and ADS results in Figure 10 at lower frequency is because the ADS parameters are designed for strong resonance only, which is below -10 dB. The effects of slot length on the R_r , L_r and C_r of the radiating elements are depicted in Table 4. It is noticed that R_r decreases by increasing slot length, and an antenna array achieves the best bandwidth ($S_{11} < -10$ dB) when the value of R_r is less than 100 ohms.

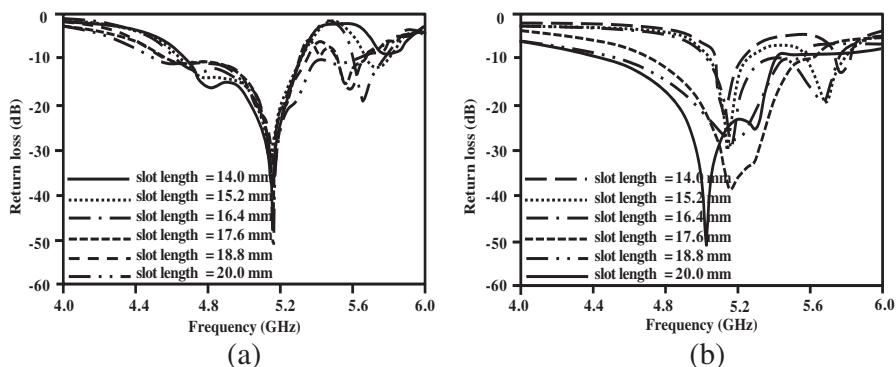


Figure 12. Slot length analysis on an array (a) CST, (b) ADS.

Table 4. Slot length effects on R_r , L_r and C_r for top, bottom and middle radiating element.

Slot length (mm)	R_r (Ohms)			L_r (pH)			C_r (pF)		
	Top Element	Bottom Element	Middle Element	Top Element	Bottom Element	Middle Element	Top Element	Bottom Element	Middle Element
14.0	120	100	58	24.059	31.375	71.5579	41.1842	24.01	13.2948
15.2	150	70	58	209.271	50.416	71.7804	48.2229	15.362	13.3361
16.4	100	53	58	40.652	44.947	89.6558	18.7315	17.716	10.6606
17.6	80	65	58	66.255	58.081	307.699	11.8501	14.153	3.29285
18.8	75	65	57	56.032	45.672	453.591	14.4668	18.549	2.23375
20	75	55	55	46.941	27.017	455.319	17.6838	32.152	2.22527

The R_r , L_r and C_r of the radiating elements are determined by using the Matlab programs of Equations (4a) to (14). For the inter-slot distance analysis, the best distance between two slots is 25 mm. Other vales of inter-slot distance on bandwidth can be seen in Table 5.

The simulated and measured E -plane ($\theta = 0^\circ$) and H -plane ($\theta = 90^\circ$) radiation patterns at 5.0 GHz and 5.6 GHz are depicted in Figure 13. The magnitude of E -plane and H -plane at 5.0 GHz is 8.3 dBi in the direction of 0° and 2° , respectively. The corresponding magnitude at 5.6 GHz is 10.5 dBi in the direction of 0° and 1° , respectively. The achieved directivity of the proposed array for 5.0 GHz is varied from 7.33 to 10.5 dBi. The simulated and measured directivities at 5.6 GHz are 10.5 dBi and 10.8 dBi, respectively. The side lobe levels using two and three slots are depicted in Figure 14(a).

Table 5. Effect of inter-slot distance on bandwidth.

Distance (mm)	Bandwidth (GHz)
23.5	0.930
24.0	0.924
24.5	0.920
25.0	1.076
25.5	0.822

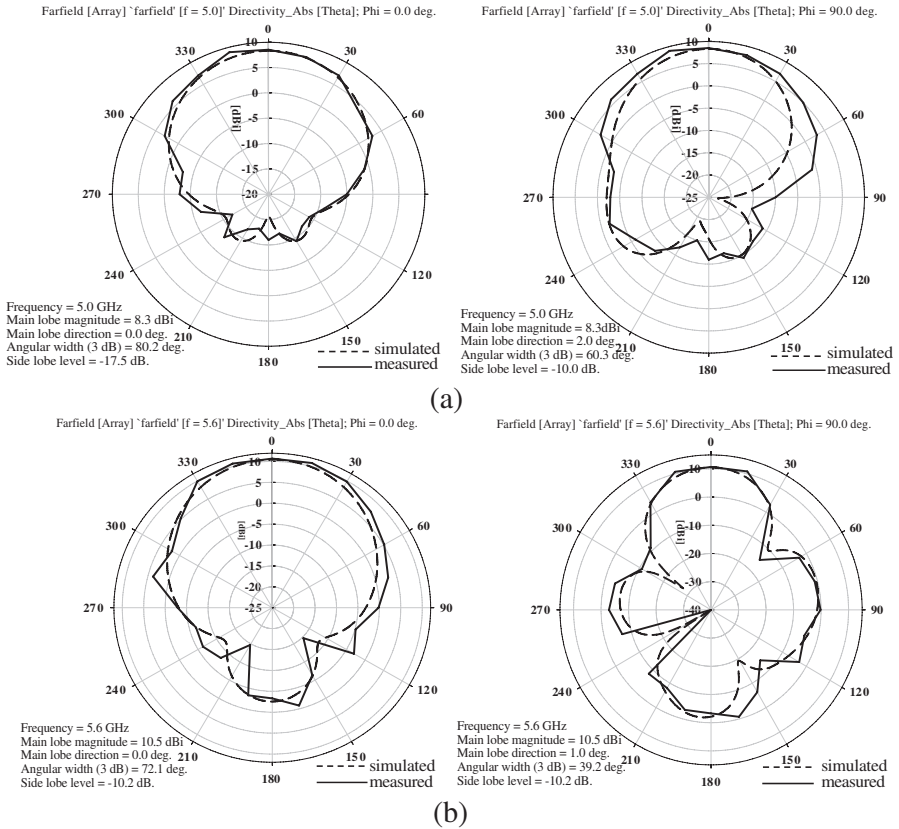


Figure 13. *E*- and *H*-plane radiation pattern at (a) 5.0 GHz, (b) 5.6 GHz.

The side-lobe levels at 5.0 GHz using two and three aperture slots are -17.6 dB and -12.4 dB, respectively. It is analyzed that using the mutual coupling mechanism in place of the third slot for this proposed array not only increases the bandwidth and gain but also reduces the side-lobe levels for whole 5.0 GHz band. The S_{11} results of the proposed array using two and three slots are depicted in Figure 14(b) which proves the advantages of using two slots and three CDRs. The comparison between the previous literatures on aperture coupled technique and the proposed work using aperture and mutual coupling is depicted in Table 6. It is clear that by utilizing aperture and mutual coupling in the proposed antenna array, the bandwidth and gain are enhanced, and the number of elements is also reduced.

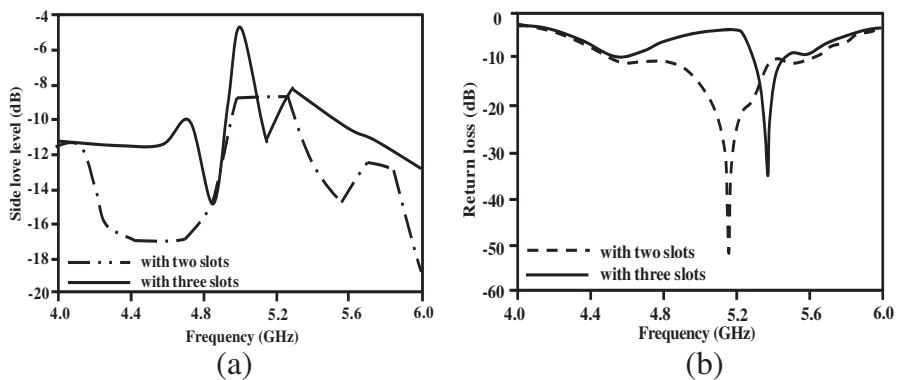


Figure 14. Comparison between two slots and three slots results. (a) Side lobe level, (b) return loss result.

Table 6. Comparison between the previous literatures on aperture coupled array antenna and the proposed array antenna.

Published work	Frequency band (GHz)	Number of elements	Bandwidth (GHz)	Maximum Gain (dBi)
M. F. Ain et al. 2012 [7]	X-band	1×4	0.042	9.0
M. F. Ain et al. 2010 [16]	5.0	3×3	0.08	10
Proposed work	5.0	1×3	1.2	10.8

5. CONCLUSION

In this paper, a lumped-element model of aperture and mutually coupled cylindrical DRA array at 5.0 GHz band is presented. In this electrical model, each array element is represented by its equivalent RLC circuit and used to predict the return loss behavior of the array. The coupling between the antenna elements are evaluated by introducing a coupling capacitor between the equivalent circuits of array elements. The numerical part of the proposed electrical model can be evaluated without using difficult mathematical programming techniques. The technique has shown its ability to generate reasonable results in all verified cases. The return loss results obtained from CST, ADS, and E8363C vector network analyzer (VNA) are in good agreement, which shows the accuracy of the proposed antenna array and its equivalent RLC model.

ACKNOWLEDGMENT

The authors would like to thank Universiti Teknologi PETRONAS in particularly Research and Innovation Office (RIO) in providing short term internal research fund for this study.

REFERENCES

1. Long, S., et al., "The resonant cylindrical dielectric cavity antenna," *IEEE Transactions on Antennas and Propagation*, Vol. 31, 406–412, 1983.
2. Ain, M. F., S. I. S. Hassan, J. S. Mandeep, M. A. Othman, B. M. Nawang, S. Sreekantan, S. D. Hutagalung, and Z. A. Ahmad, "2.5 GHz BaTiO₃ dielectric resonator antenna," *Progress In Electromagnetics Research*, Vol. 76, 201–210, 2007.
3. Dashti, H., M. H. Neshati, and F. Mohanna, "RDRA array fed by dielectric image line with improved gain & low back radiation," *1st International Conference on Communication Engineering, Journal of Mathematics*, 2010.
4. Kumari, R., et al., "A dual band triangular shaped DRA array for WLAN/WiMAX applications," *2011 Annual IEEE India Conference (INDICON)*, 1–4, 2011.
5. Yau, D. and M. V. Shuley, "Numerical analysis of an aperture coupled rectangular dielectric resonator antenna using a surface formulation and the method of moments," *IEE Proceedings — Microwaves, Antennas and Propagation*, Vol. 146, 105–110, 1999.
6. Sreekantan, S., Y. K. Ling, Z. A. Ahmad, M. F. Ain,

- M. A. Othman, and S. I. S. Hassan, "Simulation and experimental investigators on rectangular, circular and cylindrical dielectric resonator antenna," *Progress In Electromagnetics Research C*, Vol. 7, 151–166, 2009.
7. Ain, M. F., Y. M. A. Qasaymeh, Z. A. Ahmad, M. A. Zakariya, M. A. Othman, S. S. Olokede, and M. Z. Abdullah, "Novel modeling and design of circularly polarized dielectric resonator antenna array," *Progress In Electrimagnetics Research C*, Vol. 28, 165–179, 2012.
 8. Baba, A. A., M. A. Zakariya, and Z. Baharudin, "Wideband and high gain cylindrical dielectric resonator antenna array," *Proceedings of the 7th International Conference on Ubiquitous Information Management and Communication — ICUIMC 13*, Malaysia, 2013.
 9. Baba, A. A., M. A. B. Zakariya, Z. Baharudin, M. H. M. Khir, M. Z. u. Rehman, Z. A. Ahmad, and Y. M. A. Qasaymeh, "Aperture and mutual coupled cylindrical dielectric resonator antenna array," *Progress In Electromagnetics Research C*, Vol. 37, 223–233, 2013.
 10. Ahmed, O. M. H. and A.-R. Sebak, "Mutual coupling effect on ultrawideband linear antenna array performance," *International Journal of Antenna and Propagation*, Vol. 2011, Artical ID 142581, 11 Pages, 2011.
 11. Petosa, A., *Dielectric Resonator Antennas Handbook*, 2007.
 12. Ladani, F. T. and A. Z. Nezhad, "Modeling of conical dielectric resonator by simulation at 10 GHz and comparing with the cylindrical dielectric resonator," *International Symposium on Telecommunication*, 125–128, 2008.
 13. Akhavan, H. G. and D. Mirshekar-Syahkal, "Approximate model for microstrip fed slot antennas," *Electronics Letters*, Vol. 30, 1902–1903, 1994.
 14. Ferchichi, A., N. Fadlallah, and A. Gharssallah, "A novel electrical model to an antenna array," *Journal of Engineering and Technology Research*, Vol. 3, No. 12, 321–329, Nov. 2011.
 15. Verma, A. K. and Nasimuddin, "Analysis of circular microstrip antenna on thick substrate," *Journal of Mcrowaves and Optoelectronics*, Vol. 2, No. 5, 30–38, 2002.
 16. Ain, M. F., Y. M. A. Qasaymeh, Z. A. Ahmad, M. A. Zakariya, M. A. Othman, A. A. Sulaiman, A. Othman, S. D. Hutagalung, and M. Z. Abdullah, "A novel 5.8 GHz high gain array dielectric resonator antenna," *Progress In Electromagnetics Research C*, Vol. 15, 201–210, 2010.